Mitochondrial behaviors prime the selective inheritance against harmful mitochondrial DNA mutations

Zhe Chen [1,4], Zong-Heng Wang [1,4], Guofeng Zhang [2] and Hong Xu [1,3]

[1] National Heart, Lung, and Blood Institute, National Institutes of Health, Bethesda, MD 20892

[2] National Institute of Biomedical Imaging and Bioengineering, National Institutes of Health, Bethesda, MD 20892

[3] Correspondence to: hong.xu@nih.gov

[4]These authors contributed equally to this work

Abstract

Although mitochondrial DNA (mtDNA) is prone to mutation and few mtDNA repair mechanisms exist, deleterious mutations are exceedingly rare. How the transmission of detrimental mtDNA mutations are restricted through the maternal lineage is debated. Here, we use *Drosophila* to dissect the mechanisms of mtDNA selective inheritance and understand their molecular underpinnings. Our observations support a purifying selection at the organelle level based on a series of developmentally-orchestrated mitochondrial behaviors. We demonstrate that mitochondrial fission, together with the lack of mtDNA replication in proliferating germ cells, effectively segregates mtDNA into individual organelles. After mtDNA segregation, mtDNA expression begins, which leads to the activation of respiration in each organelle. The expression of mtDNA allows the functional manifestation of different mitochondrial genotypes in heteroplasmic cells, and hence functions as a stress test for each individual genome and sets the stage for the replication competition. We also show that the Balbiani body has a minor role in mtDNA selective inheritance by supplying healthy mitochondria to the pole plasm. The two selection mechanisms may act synergistically to secure the transmission of functional mtDNA through *Drosophila* oogenesis.

Introduction

Mitochondria, the indispensable power plants of eukaryotic cells, present geneticists with a fundamental paradox. Their genome accumulates mutations at a high rate in the soma, estimated to be two orders of magnitude higher than that of the nuclear genome (Wallace and Chalkia, 2013). This rate owes to both the abundance of highly-mutagenic free radicals generated by respiration and the lack of effective DNA repair *via* homologous recombination in the mitochondrial matrix (Taylor and Turnbull, 2005). If freely transmitted, the damaging mutations would gradually accumulate over generations, and eventually cause the total meltdown of mitochondrial DNA (mtDNA) (Felsenstein, 1974). However, damaging mtDNA mutations are exceedingly rare in populations. This paradox underscores the existence of effective mechanisms that restrict the transmission of deleterious mtDNA mutations and favor the selective inheritance of healthy mitochondrial genomes. Since mtDNA is predominantly transmitted through the maternal lineage, these mechanisms must operate in the female germline.

Currently, the dominant dogma, bottleneck inheritance proposes that only a small fraction of the mitochondrial genomes present in primordial germ cells are transmitted to an oocyte and eventually populate the offspring. This process explains the rapid genetic drift of mitochondrial genotypes between generations (Hauswirth and Laipis, 1982) (Olivo et al., 1983) (Rebolledo-Jaramillo et al., 2014), although how it is generated remains elusive. Bottleneck inheritance could also indirectly lead to the counterselection of deleterious mtDNA mutations: different mtDNA compositions would generate different metabolic outputs in developing oocytes, eventually causing the elimination of oocytes harboring an excess of deleterious mutations (Jenuth et al., 1996). However, the frequency of spontaneous mtDNA mutations is about 10^{-5}-10^{-6} (9), which, while high compared to the frequency of nuclear DNA mutations, remains too low to elicit the kind of biochemical deficiency required for an effective selection at the whole-cell level. In fact, deleterious mtDNA mutations are prevented from passing to the next generation even when present in low copy-number in mouse models (Stewart et al., 2008b) (Fan et al., 2008). These observations suggest that selection likely occurs at the level of

individual organelles or genomes, rather than at the level of individual cells, as implied by the bottleneck model. However, the exact mechanisms that would allow a purifying selection at the organelle level in mammals have remained unclear.

Our work in *Drosophila melanogaster* (*Dm*) has shown that selective inheritance of mtDNA also takes place in insects (Hill et al., 2014). Taking advantage of a temperature-sensitive deleterious mtDNA mutation (*mt:CoI*^{T300I}, referred to as *ts*) we had previously engineered (Hill et al., 2014), we found that the load of *ts* alleles in the progeny of heteroplasmic mothers (carrying a mix of wild-type and *ts* mtDNAs) was greatly reduced at restrictive temperature (Hill et al., 2014) . This observation suggested that the *Dm* female germline could detect the defect caused by the *ts* allele at restrictive temperature, and limit the transmission of the mtDNAs carrying it. Genetic and developmental analyses roughly mapped selective mtDNA inheritance in *Dm* to a developmental window spanning the late germarium (region 2B) and budding egg chamber stages. This is a stage where groups of 16 sister cells (16-cell cysts), derived from the four successive divisions of single oocyte precursors, organize into egg chambers from which a single egg will emerge. Interestingly, this is also a stage when mtDNA replication resumes, after having been largely quiescent in the earlier, proliferating cysts stage (region 2A) (Hill et al., 2014). mtDNA replication in this region appears to depend on active mitochondrial respiration, as both pharmacological inhibition and genetic disruption of the nuclear-encoded electron-transport chain (ETC) subunits severely impair mtDNA replication (Hill et al., 2014). The *ts* mutation, which disrupts a subunit of the mitochondria-encoded ETC complex IV, also leads to greatly diminished mtDNA replication in homoplasmic germaria (carrying only the mtDNA *ts* allele) under restrictive temperature (Hill et al., 2014). We reasoned that in heteroplasmic germ cells, healthy mitochondria carrying wild-type mtDNA would replicate their DNA and propagate much more vigorously than defective ones harboring mutations that impair respiration, which would consequently reduce the proportion of mutant mtDNA in the progeny. This reasoning led us to propose a replication-competition model for selective inheritance in *Dm* (Hill et al., 2014).

While logically compelling, the replication-competition model rests on the assumption

that germ cells can discern the integrity of individual mitochondrial genomes, presumably based on their functionally distinct protein products. However, mitochondria are not stationary: they undergo constant fusion and fission, which mixes and reassorts mitochondrial genomes and their products (Frank et al., 2001) (Ishihara et al., 2006) (Legros et al., 2004). In heteroplasmic cells, mitochondrial fusion allows mtDNA complementation to maintain the overall metabolic output in spite of significant levels of mtDNA mutations (Chan, 2006). This process could therefore mask the functional deficiency caused by deleterious mutations, and prevent the elimination of defective genomes. Therefore, we propose that mitochondrial genomes have to be effectively segregated, and then expressed, for replication-competition to lead to selective mtDNA inheritance. However, currently, it is not clear whether and how mtDNA segregation and expression are regulated during oogenesis, nor do we know how such regulation impacts mtDNA transmission and selective inheritance.

Aside from replication-competition and bottleneck inheritance, another mechanism has also been proposed, based on the observed localization and transport of mitochondria to the prospective germ plasm during oogenesis (Cox and Spradling, 2003). At the beginning of oocyte differentiation, a fraction of mitochondria and other organelles congregate within a structure called the Balbiani body, which supplies mitochondria to the pole plasm of the mature oocyte, the cytoplasm of the future embryo's primordial germ cells. It has been proposed that healthy mitochondria might be enriched in the Balbiani body and preferentially transmitted to grandchildren (Cox and Spradling, 2003). However, this idea still lacks direct experimental support. Since we have shown that selective inheritance was detectable as early as in the offspring of heteroplasmic mothers, not just in their grandchildren, this mechanism could not alone explain selective inheritance. Nevertheless, it might be an important contributor.

In this paper, we test the basic assumptions of our replication-competition model by documenting the behavior of mitochondria and their genomes in the developing *Dm* ovary. In addition, we examine the potential contribution of mitochondrial aggregation around the Balbiani body to selective mtDNA inheritance in *Dm*. Finally, we revisit the

notion that variance in heteroplasmy reflects mtDNA's passage through a bottleneck in the early stages of oogenesis.

Results

Mitochondrial genomes are segregated in the proliferating cysts (region 2A) of the *Drosophila* germarium

To determine whether mitochondrial genomes segregate to separate organelles during oogenesis, we visualized mtDNAs and their distribution in the mitochondrial network of germ cells. Mitochondrial DNA is packaged into a riboprotein complex, the nucleoid, which is the actual inheritance unit for mtDNA (Chan, 2006) (Iborra et al., 2004). Mitochondrial transcription factor A (TFAM) is the major mtDNA packaging protein and a well-established marker for mtDNA nucleoids (Alam et al., 2003). We thus imaged TFAM-GFP (Zhang et al., 2016) and mitochondria in *Drosophila* ovary to assess mtDNA segregation. The TFAM-GFP signal showed as many puncta throughout the germarium and localized to mitochondria labelled by staining for ATP synthase α subunit (Figure 1A).

To further document mitochondrial behaviors in *Drosophila* germline cells, we examined mitochondrial morphology in wild-type (wt) ovaries using transmission electron microscopy (TEM) (Figure 1B, ctrl). In the anterior part of the germarium, where the germline stem cells and cystoblasts reside (region 1), some mitochondria were elongated , while others were present in smaller, rounded organelles (Figure 1B, ctrl). Mitochondria underwent a notable remodeling in the proliferating cysts (region 2A). Most of them were fragmented, suggesting more fission events in this region (Figure 1B, 1C, ctrl).

In consistent with results from TEM assay, mitochondria stained with ATP synthase α subunit in region 1 were more elongated and interconnected, while became fragmented in proliferating cysts (region 2A) (Figure 2A, ctrl). In region 1, the number of mitochondrial nucleoids, indicated as the TFAM-GFP puncta, ranged from one to three in different mitochondria. Around 56.9% of mitochondria contained two nucleoids, while 25.9% and 17.2% of mitochondria contained 1 and 3 nucleoids, respectively (Figure 2B, ctrl). On average, there were 1.9 nucleoids per mitochondrion in this region

(Supplementary Table 1). However, in region 2A, a lack of mtDNA replication, as demonstrated previously (Hill et al., 2014), in combination with increased mitochondrial fission, should promote nucleoid segregation in this region. As expected, in region 2A, 92.6% of the mitochondria contained only 1 nucleoid (Figure 2B, ctrl), and the average number of nucleoids per mitochondrion was reduced to 1.1 (Supplementary Table 1), indicating that nucleoids are effectively segregated through mitochondrial fission in proliferating cysts before the onset of mtDNA replication in the germarium 2B region.

It has been estimated that a nucleoid may contain 1-10 copies of mtDNA, depending on cell type and tissue (Kukat et al., 2011; Legros et al., 2004; Satoh and Kuroiwa, 1991). Although mtDNA in separate nucleoids do not intermix (Gilkerson et al., 2008), those within a nucleoid can functionally complement each other, which could interfere with selective inheritance (Hill et al., 2014). Currently, there is no reliable technique to accurately quantify mtDNA copy number within a specific nucleoid. But this number can be approximated by normalizing the total number of mitochondrial genomes to the number of nucleoids in a cell. To this end, we expressed a GFP construct specific to germ cells (Vasa-GFP) and isolated germ cells by FACS (Fluorescence Activated Cell Sorting) from the ovary of white pupae. At this stage, oogenesis has progressed to region 1 of the germarium, which consists mainly of germline stem cells (GSCs) and cystoblasts (Figure 3A). We quantified the mtDNA copy number using digital PCR, a method for absolute quantification of nucleic acids. There were ~108 copies of mtDNA in GSCs and early cysts. Since there were approximately 85 nucleoids in GSCs (Figure 3B, E pupa), each nucleoid contained 1.3 copies of mtDNA on average. This number suggests that intra-nucleoid complementation is rather minimal at this stage. In addition, given that there is no mtDNA replication until region 2B, the mtDNA copy number within a nucleoid should not increase prior to the stage when selective inheritance occurs. Taken together, our observations suggest that mtDNA molecules segregate at a ratio close to one molecule per organelle during the early stages of ovarian development.

Mitochondrial fission in proliferating cyst (region 2A) is required for mtDNA selective inheritance

To test whether mtDNA segregation was required for selective inheritance, we attempted to increase the number of nucleoids per mitochondrion by tampering with mitochondrial fission. We first genetically knocked down expression of the mitochondrial Fission 1 protein (Fis1-KD) in region 2A, using a *bam-gal4* driver specifically expressed at this stage (Chen and McKearin, 2003). We examined the effect of Fis1 knockdown on mitochondrial length using TEM analysis (Figure 1B, 1C). While the average length of mitochondria remain unchanged in region 1, it increased from 0.27 to 0.48 μm in region 2A (Figure 1C), suggesting that the knockdown of Fis1 indeed interfered with mitochondrial fission. The changes of nucleoid numbers in individual mitochondrion relative to wild type were further quantified (Figure 2A, 2B). In proliferating cyst region 2A, the number of nucleoids in each mitochondrion increased from 1.1 to 1.6 on average compared to control (Supplementary Table 1) upon Fis1 knockdown. Overall, only 50.4% of mitochondria contained a single nucleoid, compared to 92.6% in wild type (Figure 2B).

We next tested the impact of impaired mitochondrial fission on mtDNA selective inheritance in heteroplasmic flies. We assayed the load of *ts* allele in each offspring of single heteroplasmic mothers at either a permissive temperature of 18 °C or a restrictive temperature of 29 °C (Figure 2C). At any given condition, the frequency of the *ts* allele in the offspring spanned a 30% range. However, while the mean *ts* frequency in the progeny of control mothers (wild-type nuclear background) produced at 18 °C was 65.7% (50.2%-76.6% range), it decreased to 36.3% (21.9%-53.8% range) in progeny produced at 29 °C, demonstrating a clear selection against the deleterious mtDNA mutation at 29 °C. By contrast, in Fis1 RNAi flies, the load of *ts* allele in progeny produced at 29 °C ranged from 60.5% to 86.3%, only a slight decrease from the 64.7%-95.3% range detected in progeny produced at 18 °C, suggesting that the inhibition of mitochondrial fission at region 2A weakened mtDNA selective transmission.

Taken together, these observations indicate that mitochondrial fission promotes nucleoid segregation in proliferating cysts at region 2A and is required for effective mtDNA selection.

Mitochondrial activity and mitochondrial DNA expression commence in the 16-cell cyst stage (region 2B)

We hypothesize that for heteroplasmic cells to distinguish between mitochondria of different mtDNA genotypes, mitochondrial genomes have to express their ETCs to activate respiration. To test this idea, we examined the pattern of mtDNA expression in the germanium by *in situ* hybridization, using short DNA probes targeted to several mtDNA encoded mRNAs (Figure 4A), including *NADH dehydrogenase 4 (ND4)* and *cytochrome c oxidase subunit 1 (cox1)* . Moderate levels of mRNAs were detected in GSCs, but almost no signal was detected in proliferating cysts of region 2A. In the following 16-cell cyst region (region 2B), a strong mRNA signal was observed, suggesting that mtDNA expression commences at this stage (Figure 4B). We also checked the expression pattern of several ETC subunits encoded in the nuclear genome, including *NADH: ubiquinone oxidoreductase subunit B5 (NDUFB5)* and *cytochrome c oxidase subunit 5A* (*cox5A*) (Figure 4A). All these mRNAs showed an expression pattern similar to that of mtDNA-encoded mRNAs, i.e, a moderate expression in germline stem cells, no expression in proliferating cysts, and strong expression at the 16-cell cyst stage (Figure 4B). These results showed the coordinated expression of mitochondrial and nuclear genes encoding subunits of the ETC in region 2B and led us to ask whether mitochondrial respiration was also activated at this stage.

To address this question, we analyzed mitochondrial respiratory activity during germarium development, using tetramethylrhodamine methyl ester (TMRM), a dye that accumulates in polarized mitochondria (Scaduto and Grotyohann, 1999). We found that the ratio of TMRM to MitoTracker green (a marker of mitochondrial mass) was markedly increased in germanium region 2B compared to regions 1 and 2A (Figure 5A), indicating that mitochondrial respiration is low in early-stage cysts, but up-regulated at the 16-cell cyst stage. The low level of respiration in the early germarium might simply owe to a lack of ETCs. To assess the level of ETCs, we directly evaluated activities of ETCs in a colorimetric assay by incubating ovaries with substrates of succinate dehydrogenase (complex II) and cytochrome C oxidase (complex IV) (Ross, 2011). Intense brown color,

indicating that both complex II and complex IV are present and active, was evident in region 2B, but mostly absent in region 1 (Figure 5B, ctrl). This result is consistent with the mitochondrial membrane potential staining (Figure 5A), confirming that mitochondrial respiration is low in proliferating cysts, but elevated in 16-cell cysts. Given their co-occurrence, the elevation of respiration is likely due to the onset of mtDNA expression that generates ETCs in 16-cell cysts, when selective inheritance begins.

Mitochondrial activation in late germarium stage allows the selective propagation of functional mtDNA

Based on the results above, we hypothesize that mtDNA expression and the following activation of respiration may act as a stress test allowing germ cells to distinguish between mitochondria that harbor a wild-type versus a mutant mtDNA. We hence predicted that a ubiquitous disruption of mitochondrial activity in heteroplasmic flies, which would mask the deficiency of mitochondria harboring the deleterious mtDNA mutation, would impair selective inheritance. To disrupt respiration in all mitochondria, we knocked down a nuclear-encoded ETC gene, *cytochrome c oxidase subunit 5A* (*cox5A*), with an appropriate RNAi. Expressing the RNAi in wild-type ovaries drastically compromised complex IV activity in region 2B (Figure 5B, *cox5A* KD). We then knocked down *cox5* in heteroplasmic *mt:CoI*^{T300I} flies and examined selective inheritance. In control groups, the average proportion of *ts* allele in progeny produced at 18°C and 29°C was 78.1% and 56.3% respectively, demonstrating a clear selection against this deleterious mutation. In *cox5A* knockdown flies, the average proportion of *ts* allele was 84.7% at 18 °C and 79.3% at 29 °C (Figure 5C). The diminished selection against the *ts* allele indicates that active mitochondrial respiration is required for selective inheritance.

If the activation of respiration in region 2B indeed functions as the stress test for mtDNA integrity, we anticipated that improving the respiratory activity of defective mitochondria carrying deleterious mutations would also weaken selective inheritance in heteroplasmic flies. We previously showed that the ectopic expression of an alternative oxidase, AOX, that catalyzes electron transfer from ubiquinone to molecular oxygen and bypasses the

cytochrome chain reactions, completely restored the viability of *mt:CoI*^{T300I} flies (Chen et al., 2015). Expression of AOX in the ovary partially restored mtDNA replication in region 2B of homoplasmic *ts* flies raised at 29 °C, based on an EdU incorporation assay (Figure 6A, 6C). Since mtDNA replication in region 2B depends on active respiration (10), this observation confirms that AOX overexpression rescues the respiration defect of *ts* mitochondria at restrictive temperature. When we overexpressed AOX in heteroplasmic *ts* flies, we found that the *ts* allele proportion in the progeny of single heteroplasmic mothers was 63.1% at 18 °C and 56.7% at 29 °C on average. The reduction was significantly less pronounced than in control heteroplasmic flies that did not express AOX (67.4% and 43.9%, respectively; Figure 6D). This observation is consistent with a disruption of selective inheritance by AOX overexpression.

The fact that either ubiquitously disrupting or improving respiration in heteroplasmic flies can weaken selective inheritance suggests that germ cells indeed rely on the respiratory activity of individual mitochondria to gauge the integrity of their mtDNA. Based on our replication-competition model, respiratory activity would then promote selective mtDNA inheritance by allowing the wild-type mtDNA harbored by healthy mitochondria to replicate more efficiently than the mutant mtDNA harbored by respiration-defective organelles. However, the importance of mtDNA replication in selective inheritance has so far not been tested.

To directly test whether mtDNA replication is required for selective inheritance, we attempted to inhibit mtDNA replication in heteroplasmic flies. We found that an RNAi against mitochondrial single-stranded DNA binding protein (mtSSB), an essential factor for mtDNA replication, markedly reduced mtDNA replication in region 2B of wild-type germaria, while mtDNA replication in other regions appeared unaffected (Figure 6B). This result indicates that knocking down *mtSSB* only moderately disrupts mtDNA replication, except in region 2B, consistent with the previous finding that mtDNA replication in region 2B is particularly sensitive to mitochondrial disruption (Hill et al., 2014). Importantly, knocking down *mtSSB* in heteroplasmic flies greatly diminished selective inheritance, as the average heteroplasmic level in the progeny of single

mothers was the same at 18 °C and 29 °C (33.1% and 32.9%, respectively; Figure 6E). This result suggests that mtDNA replication in region 2B is indeed necessary for selective inheritance.

Taken together, the results described above suggest that activation of mitochondrial respiration serves as a stress test that identifies healthy mitochondria and promotes the replication of their mtDNA.

Balbiani body makes a small contribution to selective inheritance in germ cells

So far, we have shown that mtDNA molecules become segregated to single organelles before region 2B and begin expressing their genes and replicating in region 2B. In a heteroplasmic background, these concerted behaviors presumably allow the healthy mitochondria containing wild-type mtDNA to outcompete the defective mitochondria harboring deleterious mutations in developing germ cells, which effectively reduces the proportion of mtDNA mutations in mature oocytes.

However, a developmentally-regulated localization and transport of mitochondria in the germarium has also been proposed to contribute to mtDNA selection (Cox and Spradling, 2003). In 16-cells cysts, healthy mitochondria are preferentially transported to the Balbiani body, which furnishes the pole plasm, the cytoplasm of the future embryo's primordial germ cells (PGCs). Thus, one would expect the PGCs of an embryo to have a lower level of mtDNA mutations than its somatic cells. To test this idea, we isolated PGCs from the fertilized eggs of heteroplasmic flies expressing a germ cell specific reporter, Vasa-GFP, by fluorescence-based cell sorting, and compared levels of the *ts* allele in PGCs and somatic cells. At 29 °C, the proportion of *ts* genomes in PGCs was slightly, but consistently, lower than in somatic cells in the same batch of embryos (Figure 3C, ctrl). The difference in heteroplasmic level between PGCs and somatic tissues was about 3% on average (Figure 3C, ctrl). To confirm that this difference results from an enrichment for healthy mitochondria in the Balbiani body, we performed the same experiment in the context of a germline-specific knockdown of *milton,* the adaptor that mediates the Kinesin-dependent transport of mitochondria to the Balbiani

body (Cox and Spradling, 2006). We found that the load of *ts* allele was the same in PGCs and somatic cells (Figure 3C, *milton*-KD), suggesting that a Balbiani body-associated selection of mitochondria does take place. This selection plays a complement role to further improve mitochondrial fitness in germ cells and may act synergistically with other mechanisms to further enhance the selective transmission of mtDNA in *Drosophila*.

Variance in offspring heteroplasmy reflects random genetic drift in the mother rather than a genetic bottleneck

Although the transmission of the *ts* allele from heteroplasmic mothers to their offspring is always hampered at restrictive temperature, the frequency of the *ts* allele in the offspring of single heteroplasmic mothers typically spanned a 30% range (Figure 2C, 5C, 6D, 6E). This observation suggests that each oocyte inherits a different load of mutant mtDNA. Since it has been proposed that mtDNA underwent a genetic bottleneck in other systems, we asked whether a bottleneck could take place in *Dm* as well, and explained the heteroplasmy variance in the offspring of heteroplasmic mothers. In the proliferating cysts of adult germaria (region 2A), the absence of mtDNA replication (Hill et al., 2014), greatly reduces mtDNA copy number per germ cell at the 16-cell stage. However, all mitochondria from the 16-cell cyst derived from a single cystoblast end up in the oocyte (Ganguly et al., 2012). Thus, the lack of mtDNA replication in proliferating cysts should not be mistakenly considered as a way to generate bottleneck. A potential mitochondrial bottleneck could only occur before the cystoblast. Therefore, we investigated mtDNA segregation at earlier stages of *Drosophila* oogenesis.

We determined mtDNA copy number from PGCs isolated with Vasa-GFP based cell sorting at each corresponding stage. The average mtDNA copy number per PGC/ germline stem cell gradually descended from ~340.6 in embryonic stage to ~108.4 in early pupae (Figure 3B). However, mitochondrial nucleoids, the actual inheritance units usually contain more than one copy of mtDNA. We next determined the numbers of nucleoids in PGCs from late embryonic stage to early pupa using TFAM-GFP. We found that the numbers of nucleoids were relatively constant throughout PGC

development, with approximately 80 nucleoids per cell on average (Figure 3B). Our result is consistent with a recent study determining the number of mtDNA foci based on in-situ hybridization (Hurd et al., 2016), demonstrating a lack of obvious mitochondrial bottleneck in *Drosophila*.

We next tested whether genetic drift could account for the variable segregation of ts mtDNAs to oocytes. To this end, we measured the level of heteroplasmy in the progeny of 20 individual mothers with different heteroplasmic levels (Supplementary Table 2), and used the data to calculate the number of mtDNA segregation units that would account for the observed heteroplasmy variance, using two mathematical algorithms modelling random segregation. We found that the observed number of nucleoids, approximately 80, indeed fell within the range of segregation unit numbers (50 to 300) derived from our models (Supplementary Table 3). These results suggest that there is no obvious mitochondria bottleneck in *Dm* germline, and that random segregation may account for the observed mtDNA genetic variance.

Discussion

In this study, we illustrate a series of developmentally-orchestrated mitochondrial behaviors in *Dm* germarium, including mitochondrial fission in proliferating cysts, mtDNA expression and ETCs activation in 16-cells cysts, that are indispensable for restricting the transmission of deleterious mtDNA mutations (Figure 7). In early germarium, mitochondria undergo a drastic morphological change transitioning from elongated, tubular networks in region 1, to smaller, rounded organelles in region 2A. This mitochondrial morphological change and its role in the mtDNA selective inheritance have also been demonstrated in a recent study (Lieber et al., 2019). The mitochondrial fission, together with the lack of mtDNA replication in proliferating cysts, effectively segregates mitochondrial genomes. We also estimate that each nucleoid contains ~1.3 copies of mtDNA molecules on average at this stage. Therefore, the chance of potential complementation among different mitochondrial genomes is minimized. In proliferating cysts, when mtDNA segregation takes place, mtDNA is not actively transcribed. Progressing into 16-cell cysts, mtDNA expression is activated, which triggers the biogenesis of ETCs and the activation of mitochondrial respiration. In heteroplasmic germ cells, mtDNA expression acts as a stress test for the integrity of mitochondrial genome. Mitochondria harboring wild type genome will have functional ETCs and active respiration, whereas mitochondria containing deleterious mutations have defective ETCs and impaired respiration. At region 2B, mtDNA replication resumes, and preferentially takes place in healthy mitochondria (Hill et al., 2014) . As a result, the proportion of wild type genome increase through oogenesis. It is known that many nuclear-encoded mitochondrial proteins including several key factors required for mtDNA replication, are synthesized locally on mitochondrial surface by cytosolic ribosomes (Zhang et al., 2016). This local translation allows coupling of synthesis and import of mitochondrial proteins. The import of preproteins across mitochondrial inner membrane requires mitochondrial membrane potential, which depends on active mitochondrial respiration (Geissler et al., 2000). We also found that local translation also preferentially takes place on healthy, polarized mitochondria (Zhang et al., 2019). Therefore, unhealthy mitochondria, due to the impaired local translation and import, will be starved of nuclear-encoded factors that are essential for mitochondrial biogenesis

and mtDNA replication. This may underlie, or at least contribute to, the selective replication of wild-type genomes.

We previously found that mtDNA replication commences in the 16-cell cysts, and is dependent on mitochondrial respiration. Hence, we proposed a model of selective inheritance through replication competition, in which healthy mitochondria containing a wild-type genome proliferate much more vigorously and outcompete these harboring deleterious mutations. This model explains the gradual decline of the load of deleterious mutations over generations. In mouse models, mutations on protein-coding genes that severely affect the mitochondrial respiratory chain activity were eliminated much faster than mild mutations on tRNA genes (Stewart et al., 2008a; Stewart et al., 2008b). This observation is consistent with our model of selection based on the functionality of individual genome, which might represent a conserved mechanism guiding mitochondrial inheritance in metazoans.

Other models have also been proposed to explain how harmful mtDNA mutations are restricted from transmission through the female germline. Random segregation of mtDNA, enforced by a mitochondrial bottleneck, in principle could lead to the elimination of unhealthy germ cells or individuals with an excess of damaging mtDNA mutations through Darwinian selection (Stewart and Larsson, 2014). However, it cannot explain the effective selection against low-level mtDNA mutations demonstrated in murine models and fruit flies (Stewart et al., 2008b) (Fan et al., 2008) (Hill et al., 2014) (Ma et al., 2014). In this study, we demonstrate that the number of mitochondrial nucleoids, the actual segregation units for the mitochondrial genome, remains constant from PGCs in embryo to GSCs and cystoblasts in pupae, confirming a lack of mitochondrial bottleneck in *Drosophila*. By normalizing to the number of nucleoids, we did noticed that mtDNA copy number per nucleoid decreased from 5.6 in embryonic stages to 1.3 in early pupal stage. This reduction of mtDNA copy number within a nucleoid through germline development might prepare for the effective mtDNA segregation in adult germarium. It may act synergistically with the fission-dependent mtDNA segregation in region 2A

gemarium, to minimize potential complementation among different mtDNA genotype, and therefore facilitate selective inheritance on the level of individual genome.

We also found that a proportion of healthy mitochondria in the oocytes is pre-selected to join the Balbiani body, which eventually populates germ plasm in developing embryos. Thus, the Balbiani body enforces another purifying selection to further enhance mitochondrial fitness specifically in germ cells of offspring. The exact mechanism of how the healthy mitochondria are predetermined and unevenly distributed in the oocyte is unclear. Given the essential role of Milton in the formation of Balbiani body and mtDNA selective inheritance, it is possible that the healthy mitochondria are preferentially transported along the microtubules to Balbiani body, and then localized to the posterior end of oocytes. Balbiani body is a conserved structure in developing oocytes of several different species (Pepling et al., 2007) (Zhou et al., 2010) (Cox and Spradling, 2003) (Tworzydlo et al., 2016). Its role in mitochondrial inheritance, particularly selective inheritance against damaging mtDNA mutations, remains to be explored in flies and other organisms.

Methods

Drosophila genetics

Flies were maintained on cornmeal medium at 25 °C, unless otherwise stated. *w* ^{1118} was used as the wild-type control. Heteroplasmic *mt:CoI*^{T300I} flies were generated as described previously (Hill et al., 2014), and maintained at 18 °C, unless otherwise stated. Generation of the Tfam-gfp reporter lines and transgenic flies expressing alternative oxidase UAS-AOX was described previously (Zhang et al., 2016) (Chen et al., 2015). Fis1 RNAi (BL#63027), cox5A RNAi (BL#58282), mtSSB RNAi lines (BL#50600), X-linked mChFP-Rho1(BL#52280), Bam-gal4 (BL#80579), nanos-gal4 (BL#4937) came from the Bloomington *Drosophila* Stock Center (Bloomington, IN). Vasa-GFP (#109171) came from the Kyoto Drosophila Genomics and Genetics Resources.

Immunostaining of *Drosophila* germ cells

For staining of adult ovaries, 1-to-2-day old females were fed with yeast overnight prior to analysis. Ovaries were dissected in Schneider's medium supplemented with 10% fetal bovine serum (FBS, Gibco) at room temperature. The female 3rd instar larval and pupal ovaries are tiny and embedded in the fat body, so they remain attached to the fat body during staining. Ovaries were fixed for 20 minutes in 3.7% paraformaldehyde (Electron Microscopy Sciences) in PBS, then permeabilized in PBS containing 0.5% Triton-X100. After blocking in the PBSBT buffer (1 x PBS, 0.1% Triton-X100, 0.2% bovine serum albumin, BSA), the ovaries were incubated with primary antibodies overnight at 4 °C. Following washing with PBSBT buffer for three times, the ovaries were incubated with secondary antibodies at room temperature for 1 hr and washed again with PBSBT buffer for three times. For adult ovaries, each ovariole was separated with fine-nose forceps under the stereomicroscope and mounted with Vectashield mounting medium (Vector Laboratories) on the slides. The 3rd- instar larval and pupal ovaries were separated from the fat body before mounting.

The late-embryonic and early-larval (1st and 2nd instar larval) stage *Drosophila* gonads were stained *in situ* in whole animals as described previously (Fidler et al., 2014). Of

note, to facilitate penetration of antibodies through the cuticle, the late embryos, 1st instar and 2nd instar larvae were sonicated 2, 5, and 15 times, respectively.

All images were collected on a Perkin Elmer Ultraview system and processed with Volocity software. The number of mitochondrial nucleoids per mitochondrion was quantified by manually identifying the nucleoid numbers, indicated as the TFAM-GFP puncta within one mitochondrial fragment.

Antibodies used were as follows: mouse α□ATP synthase subunit α (Abcam, 15H4C4, 1:1,000), Rat α□Vasa (Developmental Studies Hybridoma Bank, DSHB, 1:200), Alexa Fluor 568 goat α□Rat IgG (Invitrogen, 1:200), Alexa Fluor 568 goat α□mouse IgG (Invitrogen, 1:200), Alexa Fluor 568 goat α□rabbit IgG (Invitrogen, 1:200).

Transmission electron microscopy (TEM) and quantification

Ovaries were dissected in Schneider's medium supplemented with 10% fetal bovine serum (FBS, Gibco), and immediately fixed in fixation solution (2.5% glutaraldehyde, 2% formaldehyde, 2 mM calcium chloride in 0.1 M sodium cacodylate buffer) at room temperature for 5 min, followed by an additional fixation on ice for 3 hr. After washing in cold cacodylate buffer containing 2 mM calcium chloride, the ovaries were post-fixed with reduced 2% Os_2O_4 (reduced by 1.5% potassium ferrocyanide right before use) for 1 hr on ice. Following washing with water, the tissues were placed in the thiocarbohydrazide (TCH) solution for 20 min at room temperature. Then, the ovaries were fixed in 2% Os_2O_4 for 30 min at room temperature, *en bloc* stained with 1% uranyl acetate overnight at 4°C, and further stained with Walton's lead aspartate solution for 30 min at 60°C. After dehydration with ethanol series, the samples were embedded in Durcupan ACM resin (EMS). The 8-nm thin sections were viewed on a Tecnai T12 (FEI, Hillsboro, OR) transmission electron microscope.

The mitochondrial length in TEM images were analyzed with NIH ImageJ software. Individual mitochondrion from germ cells in indicated regions was manually outlined with

"freehand selections". The max ferret diameter was considered as length of the mitochondrion.

Membrane potential staining

Adult ovaries were dissected in Schneider's medium supplemented with 10% fetal bovine serum (FBS, Gibco) and incubated with medium containing Tetramethylrhodamine (TMRM, Invitrogen, 1:1000) and mitoTracker Green (Invitrogen, 100 nM) for 20 min. The ovaries were rinsed with PBS for 3 times, and then imaged live on a Perkin Elmer Ultraview system within 1 hr.

Mitochondrial activity staining and EdU labelling of *Drosophila* adult ovaries

Histochemical staining for the activity of mitochondrial succinate dehydrogenase (complex II) and cytochrome C oxidase (complex IV) in ovaries was performed as previously described (Ren et al., 2017). EdU incorporation assay in *Drosophila* ovaries was carried out as described (Hill et al., 2014).

RNA in situ hybridization

The mtDNA expression pattern in the germarium was detected using a single-molecule fluorescence *in situ* hybridization (smFISH) protocol published previously (Trcek et al., 2017). The sequence of fluorescently labelled short DNA probes targeting to *ND4*, *cox1*, *NDUFB5* and cox5A mRNA are listed in Supplementary Table 4.

Primordial germ cell isolation from *Drosophila*

The primordial germ cells from *Drosophila* embryos, larvae and pupae were isolated as previously described (Shigenobu et al., 2006) with modification. A Vasa-GFP transgene that specifically labels germ cells throughout the life cycle was used to isolate the germ cells using fluorescence-activated cell sorting (FACS) assay. Female PGCs were separated from male PGCs by an X-chromosome linked monomeric cherry fluorescence (mChFP) tagged Rho1 protein under control of Rho1 regulatory sequence (Abreu-Blanco et al., 2014). The female X-linked mChFP-Rho1 flies, which carry wild-type or heteroplasmic *mt:CoI*^{T300I} mtDNA, were crossed with male Vasa-GFP

transgenic flies in cages and allowed to lay eggs on a grape agar plate (Genesee Scientific. Inc). The germ cells of the female progeny will carry both GFP and mChFP fluorescence. Following pre-collection for 3 hr, the embryos were collected and allowed to develop till stage 15 at 25 °C (staging according to (Williamson and Lehmann, 1996)). The embryos were then dechorionated for 30 s in 50% bleach. After washing with water, the embryos were transferred to a microcentrifuge tube filled with 500 µl of Schneider's insect medium (Gibco). The blue pestle matching with the microcentrifuge tube (USA Scientific, Inc.) was used to gently homogenize the embryos. The homogenate was filtered through a 125 µm mesh and then centrifuged at 860 g for 1 min at 4 °C. After one wash in ice-cold calcium-free Schneider's medium (Sigma), the pellet was resuspended in calcium-free Schneider's medium containing 0.25% trypsin (Invitrogen) and incubated at 37°C for 10 min. The cell suspension was filtered through a 35 µm mesh, and the same amount of Schneider's medium supplemented with 20% fetal bovine serum (Gibco) was added to stop the trypsinization. The dissociated cells were pelleted by centrifugation at 860 g for 1 min. The cells were resuspended in Schneider's medium and filtered through a 35 µm mesh immediately before cell sorting. Flow cytometry analyses were performed on a BD FACSCalibur flow cytometer and analyzed with FACSDiva. The female PGCs were sorted by gating for GFP and mChFP-positive events. Female somatic cells were sorted by gating for GFP-negative and mChFP-positive events. The quality and purity of the sorted PGCs were confirmed by fluorescence microscope. For isolation of PGCs from larvae and pupae, the staged embryos were transferred to the standard cornmeal medium till the desired development stage. All the other procedures were the same except for the exclusion of the dechorionation step.

Measurement of mtDNA copy number

To quantify mtDNA copy number, total DNA was isolated from the FACS-sorted PGCs or the somatic cells using QIAamp DNA Micro Kit (Qiagen). The mtDNA copy number was measured using droplet digital PCR (ddPCR, Bio-rad), a method for absolute quantification of nucleic acids. Primers were targeted to the mtDNA-encoded

cytochrome c oxidase subunit I (CoI), and the nuclear-encoded Histone 4 (His4) genes. Primers and probes used in ddPCR are as follows:

CoI-forward: 5'ATTGGAGTTAATTTAACATTTTTTCCTCA3'

CoI-rev: 5'AGTTGATACAATATTTCATGTTGTGTAAG3'

CoI-probe: 5'AATACCTCGACGTTATTCAGATTACCCA3'

His4-for: 5'TCCAAGGTATCACGAAGCC3'

His4-rev: 5'AACCTTCAGAACGCCAC3'

His4-probe: 5'AGCGCATATCTGGACTCATATACGAG3'.

The CoI-probe and His4-probe were synthesized by labeling the 5' nucleotide with FAM and HEX reporter fluorophores, respectively. Around 1 µg of total DNA was digested with EcoRI at 37 °C for 1 hr. Then the ddPCR reaction mixture was assembled to contain 1x ddPCR Supermix for probes (Bio-rad), 900 nM of each forward and reverse primers, 250 nM of probe, and up to 1 ng of total DNA. The reaction was conducted in the QX200™ Droplet Generator, followed by the thermal cycler and analyzed by the QX200 Droplet reader as per the manufacturer's instruction.

Quantification of heteroplasmy

A single heteroplasmic female fly (herein called P_0) with wild type or tissue specific knockdown nuclear gene was crossed with several w^{1118} male flies in individual vials and lay eggs at 18°C. After 3-4 days, the P_0 was transferred to a new vial and incubated at 29°C for 3 days. This vial was discarded and the P_0 were allowed to lay eggs at 29°C. The progeny produced at 18°C and 29°C were collected and the heteroplasmic levels were quantified as described previously (Hill et al., 2014).

Prediction of the mitochondrial genetic segregation unit numbers

Twenty female heteroplasmic $mt{:}CoI^{T300I}$ flies with various heteroplasmic levels were crossed with several w^{1118} male flies in individual vials at 18°C. The first cohort of progeny were allowed to develop to 3rd instar larval stage at 18°C, then collected and the percentage of wild-type mtDNA in each progeny was quantified. Approximately 10 progeny from each of the 20 female flies were quantified (Supplementary Table 2) and the data was used to calculate the number of mitochondrial genetic segregation units in

the following manner.

The measurements of the mitochondrial segregation units are critically dependent on the chosen mathematical models. Here we use two mathematic models, the population genetic model (model 1) and the single-sampling binomial model (model 2) to do the calculation: Model 1: $V_n = p_A (1-p_A)[1-(1-1/N_{cd})^{kn}]$ and Model 2: $V=p_A (1-p_A)/N$. Model 1 assumes that segregation units are sampled randomly over multiple cell divisions, with daughter cells inheriting the same amount of units at each division (Jenuth et al., 1996) (Cree et al., 2008). In our particular scenario, N_{cd} is the number of segregation units at each cell division and is assumed to be a constant value for each mitochondrial sampling; V_n is the variance of heteroplasmic level at the nth generation, here we use the first-generation fly; pA and (1- pA) define the initial percentage of the wild-type and mutant mtDNA; k is the number of times mtDNA units have been randomly sampled (or the number of germ cell divisions). In *Drosophila* (Solignac et al., 1987), there are 12-18 pole cells at embryonic stage 10, which undergo around 2-3 divisions until stage 14, where there are 36-44 pole cells. During invagination process, those pole cells which do not migrate to the gonad degenerate. Around 8 remaining pole cells further divide and lead to 100 stem cells in the germarium of adult ovaries, which represents another 3-4 rounds of cell divisions. The adult stem cells undergo asymmetric division to form a daughter stem cell and a cystoblast. The cystoblast divides four times with incomplete cytokinesis, to form an interconnected 16-cell blast. Only one of these 16 cells becomes an oocyte; the other 15, known as nurse cells, will eventually transfer all their cytoplasm including mitochondria to the oocyte. Therefore, the divisions subsequent to stem cell division do not lead to the segregation of mitochondria. The first cohort of progeny are usually assumed to have undergone 7 rounds of mitochondrial sampling (Ma et al., 2014). Thus, we used k=7 in our calculation in this model. However, we reason that this model might assume less variation and overestimate the real size of the segregation units for two reasons: first it assumes a symmetric segregation of mitochondria at each cell division and does not consider factors that may cause more variation, such as uneven distribution of mtDNA, random mtDNA replication and mitochondria turnover. Second, this model does not consider that a large proportion of pole cells are lost during

migration, which might introduce more variation. As a result, this model may underestimate variations and lead to bigger segregation unit numbers than there actually are.

Model 2 describes the whole process and assumes a single random sampling of mtDNA molecules during oogenesis (Cree et al., 2008) (Bendall et al., 1996). In this model, N is the estimated effective segregating unit number; V is the variance of the heteroplasmy of progeny; pA and (1- pA) define the same entities as above. We reason that this model may undervalue the real mitochondrial segregating unit number N, because fewer occurrences of random sampling should lead to a larger variation, thus an underestimation of N. Therefore, the real number of mitochondrial segregation units should be within the range calculated by the above two models.

To minimize the errors caused by the calculation from a single mother and her specific heteroplasmy level, we used 20 female heteroplasmic *mt:CoI*^{T300I} flies with various heteroplasmic percentages. Subsequently, we employed the following formula to correct all the data to make p_A, the initial percentage of the mtDNA variants, as 50% in each group: $P_A = (P_x - P_0)/[P_0(1-P_0)]^{1/2} + 0.5$, where Px is the percentage of mutant mtDNA of each progeny, and P0 is the initial percentage of mutant mtDNA of each group (heteroplasmic level of mother fly). The corrected values were used to calculate V and V_n.

Statistical analysis

Data were analyzed using Student's *t* test or one-way analysis of variance. The difference was considered statistically significant when $p < 0.05$.

Acknowledgements

We thank F. Chanut for comments and edits on the manuscript; the Bloomington *Drosophila* Stock Center for fly stocks; NHLBI FACS core for technical assistance. This work is supported by NHLBI Intramural Research Program.

Abreu-Blanco, M.T., J.M. Verboon, and S.M. Parkhurst. 2014. Coordination of Rho family GTPase activities to orchestrate cytoskeleton responses during cell wound repair. *Curr Biol*. 24:144-155.

Alam, T.I., T. Kanki, T. Muta, K. Ukaji, Y. Abe, H. Nakayama, K. Takio, N. Hamasaki, and D. Kang. 2003. Human mitochondrial DNA is packaged with TFAM. *Nucleic Acids Res*. 31:1640-1645.

Bendall, K.E., V.A. Macaulay, J.R. Baker, and B.C. Sykes. 1996. Heteroplasmic point mutations in the human mtDNA control region. *Am J Hum Genet*. 59:1276-1287.

Chan, D.C. 2006. Mitochondria: dynamic organelles in disease, aging, and development. *Cell*. 125:1241-1252.

Chen, D., and D.M. McKearin. 2003. A discrete transcriptional silencer in the bam gene determines asymmetric division of the Drosophila germline stem cell. *Development*. 130:1159-1170.

Chen, Z., Y. Qi, S. French, G. Zhang, R. Covian Garcia, R. Balaban, and H. Xu. 2015. Genetic mosaic analysis of a deleterious mitochondrial DNA mutation in Drosophila reveals novel aspects of mitochondrial regulation and function. *Mol Biol Cell*. 26:674-684.

Cox, R.T., and A.C. Spradling. 2003. A Balbiani body and the fusome mediate mitochondrial inheritance during Drosophila oogenesis. *Development*. 130:1579-1590.

Cox, R.T., and A.C. Spradling. 2006. Milton controls the early acquisition of mitochondria by Drosophila oocytes. *Development*. 133:3371-3377.

Cree, L.M., D.C. Samuels, S.C. de Sousa Lopes, H.K. Rajasimha, P. Wonnapinij, J.R. Mann, H.H. Dahl, and P.F. Chinnery. 2008. A reduction of mitochondrial DNA molecules during embryogenesis explains the rapid segregation of genotypes. *Nat Genet*. 40:249-254.

Fan, W., K.G. Waymire, N. Narula, P. Li, C. Rocher, P.E. Coskun, M.A. Vannan, J. Narula, G.R. Macgregor, and D.C. Wallace. 2008. A mouse model of mitochondrial disease reveals germline selection against severe mtDNA mutations. *Science*. 319:958-962.

Felsenstein, J. 1974. The evolutionary advantage of recombination. *Genetics*. 78:737-756.

Fidler, A., L. Boulay, and M. Wawersik. 2014. Sonication-facilitated immunofluorescence staining of late-stage embryonic and larval Drosophila tissues in situ. *J Vis Exp*:e51528.

Frank, S., B. Gaume, E.S. Bergmann-Leitner, W.W. Leitner, E.G. Robert, F. Catez, C.L. Smith, and R.J. Youle. 2001. The role of dynamin-related protein 1, a mediator of mitochondrial fission, in apoptosis. *Dev Cell*. 1:515-525.

Ganguly, S., L.S. Williams, I.M. Palacios, and R.E. Goldstein. 2012. Cytoplasmic streaming in Drosophila oocytes varies with kinesin activity and correlates with the microtubule cytoskeleton architecture. *Proc Natl Acad Sci U S A*. 109:15109-15114.

Geissler, A., T. Krimmer, U. Bomer, B. Guiard, J. Rassow, and N. Pfanner. 2000. Membrane potential-driven protein import into mitochondria. The sorting sequence of cytochrome b(2) modulates the deltapsi-dependence of translocation of the matrix-targeting sequence. *Mol Biol Cell*. 11:3977-3991.

Gilkerson, R.W., E.A. Schon, E. Hernandez, and M.M. Davidson. 2008. Mitochondrial nucleoids maintain genetic autonomy but allow for functional complementation. *J Cell Biol*. 181:1117-1128.

Hauswirth, W.W., and P.J. Laipis. 1982. Mitochondrial DNA polymorphism in a maternal lineage of Holstein cows. *Proc Natl Acad Sci U S A*. 79:4686-4690.

Hill, J.H., Z. Chen, and H. Xu. 2014. Selective propagation of functional mitochondrial DNA during oogenesis restricts the transmission of a deleterious mitochondrial variant. *Nat Genet*. 46:389-392.

Hurd, T.R., B. Herrmann, J. Sauerwald, J. Sanny, M. Grosch, and R. Lehmann. 2016. Long Oskar Controls Mitochondrial Inheritance in Drosophila melanogaster. *Dev Cell*. 39:560-571.

Iborra, F.J., H. Kimura, and P.R. Cook. 2004. The functional organization of mitochondrial genomes in human cells. *BMC Biol*. 2:9.

Ishihara, N., Y. Fujita, T. Oka, and K. Mihara. 2006. Regulation of mitochondrial morphology through proteolytic cleavage of OPA1. *EMBO J*. 25:2966-2977.

Jenuth, J.P., A.C. Peterson, K. Fu, and E.A. Shoubridge. 1996. Random genetic drift in the female germline explains the rapid segregation of mammalian mitochondrial DNA. *Nat Genet*. 14:146-151.

Kukat, C., C.A. Wurm, H. Spahr, M. Falkenberg, N.G. Larsson, and S. Jakobs. 2011. Super-resolution microscopy reveals that mammalian mitochondrial nucleoids have a uniform size and frequently contain a single copy of mtDNA. *Proc Natl Acad Sci U S A*. 108:13534-13539.

Legros, F., F. Malka, P. Frachon, A. Lombes, and M. Rojo. 2004. Organization and dynamics of human mitochondrial DNA. *J Cell Sci*. 117:2653-2662.

Lieber, T., S.P. Jeedigunta, J.M. Palozzi, R. Lehmann, and T.R. Hurd. 2019. Mitochondrial fragmentation drives selective removal of deleterious mtDNA in the germline. *Nature*.

Ma, H., H. Xu, and P.H. O'Farrell. 2014. Transmission of mitochondrial mutations and action of purifying selection in Drosophila melanogaster. *Nat Genet*. 46:393-397.

Olivo, P.D., M.J. Van de Walle, P.J. Laipis, and W.W. Hauswirth. 1983. Nucleotide sequence evidence for rapid genotypic shifts in the bovine mitochondrial DNA D-loop. *Nature*. 306:400-402.

Pepling, M.E., J.E. Wilhelm, A.L. O'Hara, G.W. Gephardt, and A.C. Spradling. 2007. Mouse oocytes within germ cell cysts and primordial follicles contain a Balbiani body. *Proc Natl Acad Sci U S A*. 104:187-192.

Rebolledo-Jaramillo, B., M.S. Su, N. Stoler, J.A. McElhoe, B. Dickins, D. Blankenberg, T.S. Korneliussen, F. Chiaromonte, R. Nielsen, M.M. Holland, I.M. Paul, A. Nekrutenko, and K.D. Makova. 2014. Maternal age effect and severe germ-line bottleneck in the inheritance of human mitochondrial DNA. *Proc Natl Acad Sci U S A*. 111:15474-15479.

Ren, Q., F. Zhang, and H. Xu. 2017. Proliferation Cycle Causes Age Dependent Mitochondrial Deficiencies and Contributes to the Aging of Stem Cells. *Genes (Basel)*. 8.

Ross, J.M. 2011. Visualization of mitochondrial respiratory function using cytochrome c oxidase/succinate dehydrogenase (COX/SDH) double-labeling histochemistry. *J Vis Exp*:e3266.

Satoh, M., and T. Kuroiwa. 1991. Organization of multiple nucleoids and DNA molecules in mitochondria of a human cell. *Exp Cell Res*. 196:137-140.

Scaduto, R.C., Jr., and L.W. Grotyohann. 1999. Measurement of mitochondrial membrane potential using fluorescent rhodamine derivatives. *Biophys J*. 76:469-477.

Shigenobu, S., K. Arita, Y. Kitadate, C. Noda, and S. Kobayashi. 2006. Isolation of germline cells from Drosophila embryos by flow cytometry. *Dev Growth Differ*. 48:49-57.

Solignac, M., J. Genermont, M. Monnerot, and J.C. Mounolou. 1987. Drosophila Mitochondrial Genetics: Evolution of Heteroplasmy through Germ Line Cell Divisions. *Genetics*. 117:687-696.

Stewart, J.B., C. Freyer, J.L. Elson, and N.G. Larsson. 2008a. Purifying selection of mtDNA and its implications for understanding evolution and mitochondrial disease. *Nat Rev Genet*. 9:657-662.

Stewart, J.B., C. Freyer, J.L. Elson, A. Wredenberg, Z. Cansu, A. Trifunovic, and N.G. Larsson. 2008b. Strong purifying selection in transmission of mammalian mitochondrial DNA. *PLoS Biol*. 6:e10.

Stewart, J.B., and N.G. Larsson. 2014. Keeping mtDNA in shape between generations. *PLoS Genet*. 10:e1004670.

Taylor, R.W., and D.M. Turnbull. 2005. Mitochondrial DNA mutations in human disease. *Nat Rev Genet*. 6:389-402.

Trcek, T., T. Lionnet, H. Shroff, and R. Lehmann. 2017. mRNA quantification using single-molecule FISH in Drosophila embryos. *Nat Protoc*. 12:1326-1348.

Tworzydlo, W., E. Kisiel, W. Jankowska, A. Witwicka, and S.M. Bilinski. 2016. Exclusion of dysfunctional mitochondria from Balbiani body during early oogenesis of Thermobia. *Cell Tissue Res*. 366:191-201.

Wallace, D.C., and D. Chalkia. 2013. Mitochondrial DNA genetics and the heteroplasmy conundrum in evolution and disease. *Cold Spring Harb Perspect Biol*. 5:a021220.

Williamson, A., and R. Lehmann. 1996. Germ cell development in Drosophila. *Annu Rev Cell Dev Biol*. 12:365-391.

Zhang, Y., Y. Chen, M. Gucek, and H. Xu. 2016. The mitochondrial outer membrane protein MDI promotes local protein synthesis and mtDNA replication. *EMBO J*. 35:1045-1057.

Zhang, Y., Z.H. Wang, Y. Liu, Y. Chen, N. Sun, M. Gucek, F. Zhang, and H. Xu. 2019. PINK1 Inhibits Local Protein Synthesis to Limit Transmission of Deleterious Mitochondrial DNA Mutations. *Mol Cell*. 73:1127-1137 e1125.

Zhou, R.R., B. Wang, J. Wang, H. Schatten, and Y.Z. Zhang. 2010. Is the mitochondrial cloud the selection machinery for preferentially transmitting wild-type mtDNA between generations? Rewinding Muller's ratchet efficiently. *Curr Genet*. 56:101-107.

Figures and Figure Legends

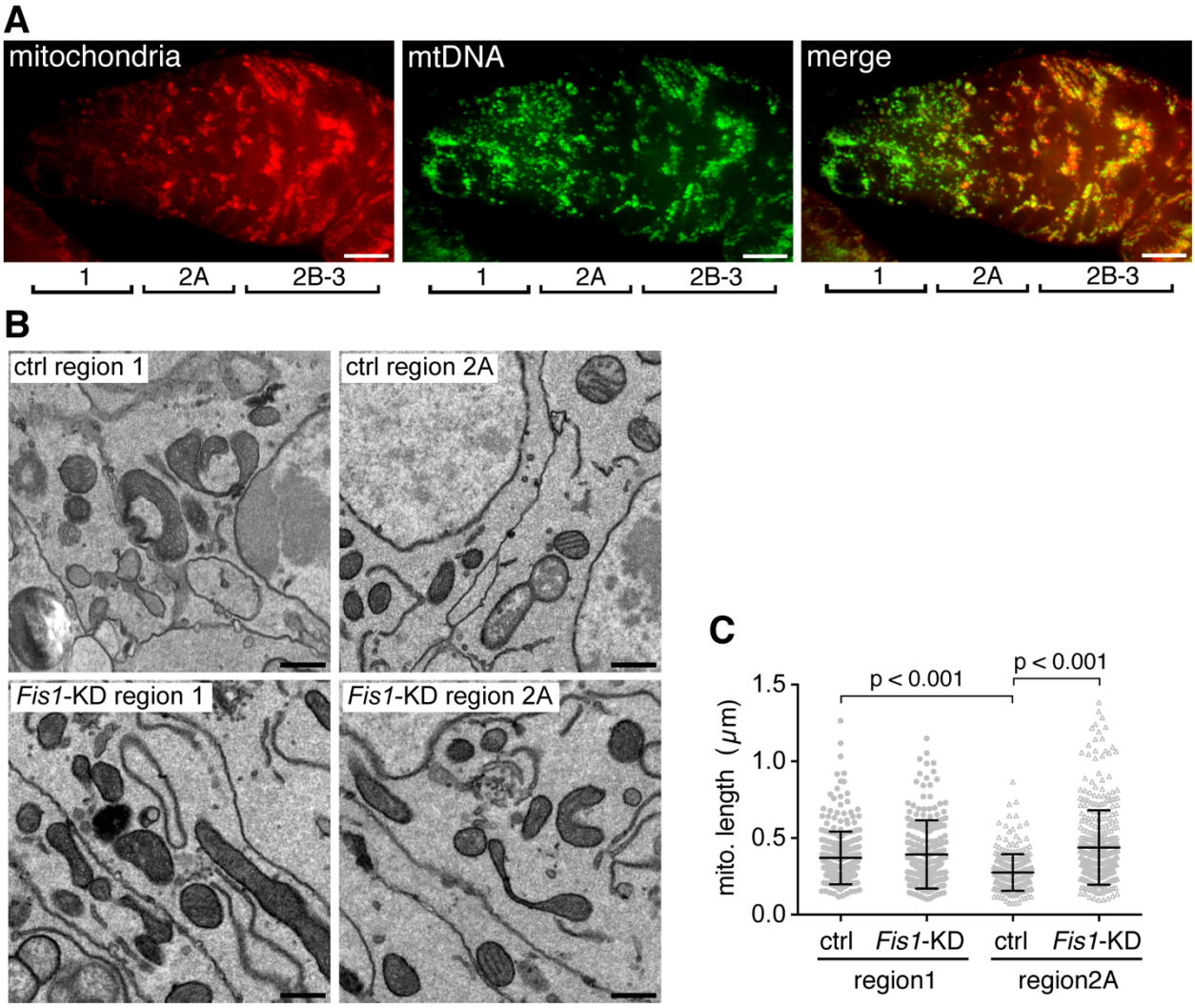

Figure 1. Mitochondria in proliferating cysts are fragmented. (A) Mitochondria and mtDNA in *Drosophila* germarium. The images are a representative *z*-stack projection of a germarium showing mitochondrial nucleoids labeled by TFAM-GFP and mitochondria labeled by ATP synthase α subunit staining. The developmental regions of germarium are indicated. Scale bar, 10 μm. (B) Mitochondria in region 1 are more elongated, while those in region 2A are fragmented. The images are electron micrographs of stem cells and cystoblasts (region 1) and proliferating cyst (region 2A) from wild-type and Fis1 knockdown germaria. The images show representative mitochondrial morphology from at least five germaria analyzed per genotype with three sections viewed for each. Scale bar, 0.5 μm. (C) The mitochondria in region 2A are

significantly elongated upon Fis1 knockdown driven by Bam-gal4 driver, as demonstrated by the length of single mitochondrion. $p<0.001$.

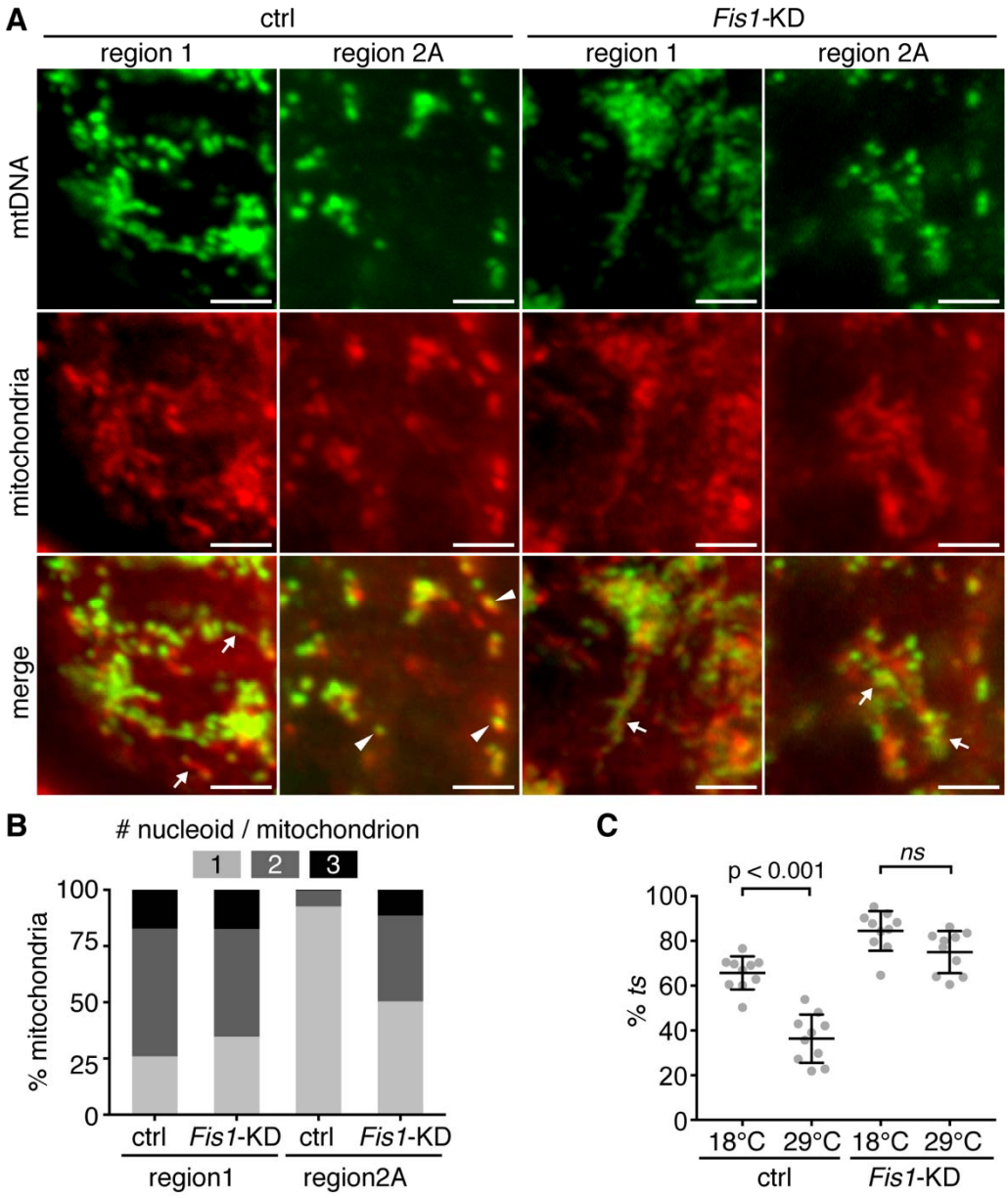

Figure 2. Mitochondrial fission and nucleoid segregation in proliferating cysts are essential for mtDNA selective inheritance. (A) Mitochondria in region 2A are elongated upon Fis1 knockdown driven by Bam-gal4, and could contain multiple nucleoids. Mitochondrial nucleoids labeled by TFAM-GFP and mitochondria labeled by ATP synthase α-subunit staining are shown in magnified views in a germarium. Arrows point to elongated mitochondria containing multiple nucleoids. Arrowheads point to fragmented mitochondria containing one nucleoid. Scale bar, 5 μm. (B) Number of nucleoids per mitochondria in

regions 1 and 2A in wild-type and Fis1 knockdown ovaries. The number of nucleoids per mitochondria were determined using TFAM-GFP and ATP synthase α-subunit staining shown in (A). (C) Knockdown of Fis1 in germarium region 2A, using a Bam-Gal4 driver, compromises the selection against the mutant mtDNA in heteroplasmic *mt:CoI*^{T300I} *Drosophila*. The proportion of mutant *ts* mtDNA in ten individual offsprings of a single heteroplasmic mother was dramatically reduced at 29°C compared to 18°C ($p<0.001$), consistent with selection against the mutant mtDNA. However, this negative selection was diminished in Fis1 knockdown fly.

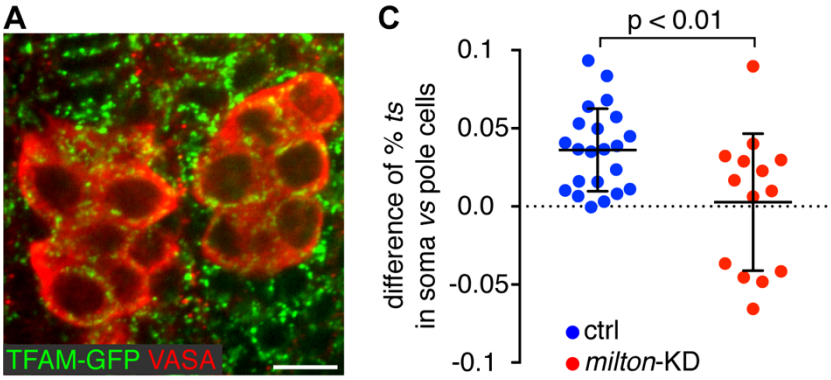

B

	# nucleoid		# mtDNA		# mtDNA / nucleoid
	mean	CV%	mean	CV%	
embryo (18)	78.1	15.5	340.6	36.5	4.4
1st larva (10)	77.0	20.5	220.4	41.1	2.9
2nd larva (7)	69.4	5.6	206.4	14.2	3.0
3rd larva (9)	107.7	10.7	166.0	14.9	1.5
E pupa (24)	85.3	16.9	108.4	27.4	1.3

Figure 3. Evolution of the number of mitochondrial genome along *Drosophila* germline development, and the contribution of Balbiani body to mtDNA selection. (A) Mitochondrial nucleoids in germ cells of early pupal stage. Nucleoids were labelled by TFAM-GFP, and *Drosophila* germ cells were stained with Vasa antibody. Scale bar, 10 μm. (B) Quantification of mitochondrial nucleoid number and mtDNA copy number in each germ cell along *Drosophila* development. E pupa, early pupal stage. CV, coefficient of variance; *n*, number of cells studied. (C) Balbiani body contributes to the selection against the *mt:CoI*^{T300I} mtDNA in the germ line of heteroplasmic flies. Somatic cells consistently have a higher percentage of *ts* mtDNA than germ cells (pole cells) in heteroplasmic embryos. Disrupting the Balbiani body by knocking down the *milton* gene (*milton-KD*) in germ cells abolishes the difference between somatic and germ cells.

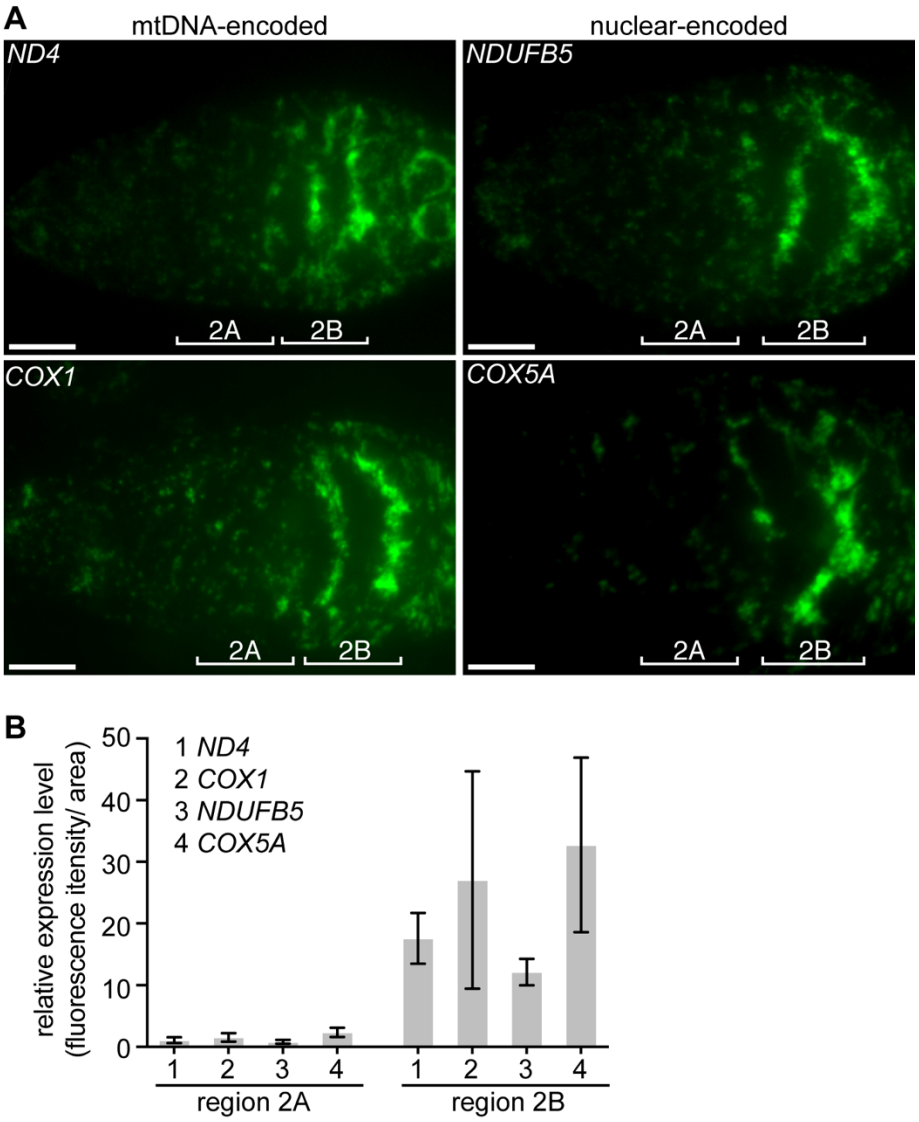

Figure 4. Expression of mtDNA- and nuclear-encoded ETCs genes in the germarium. (A) The spatial patterns of nuclear and mitochondrial encoded mRNAs were revealed by *in situ* hybridization assay. Fluorescently labelled probes targeted the mtDNA-encoded *ND4* and *cox1* transcripts, and the nuclear-encoded *NDUFB5* and *cox5A* transcripts. Scale bar, 10 μm. (B) Quantification of immunofluorescence intensity in region 2A and 2B. The expression of both types of RNAs was dramatically increased at region 2B.

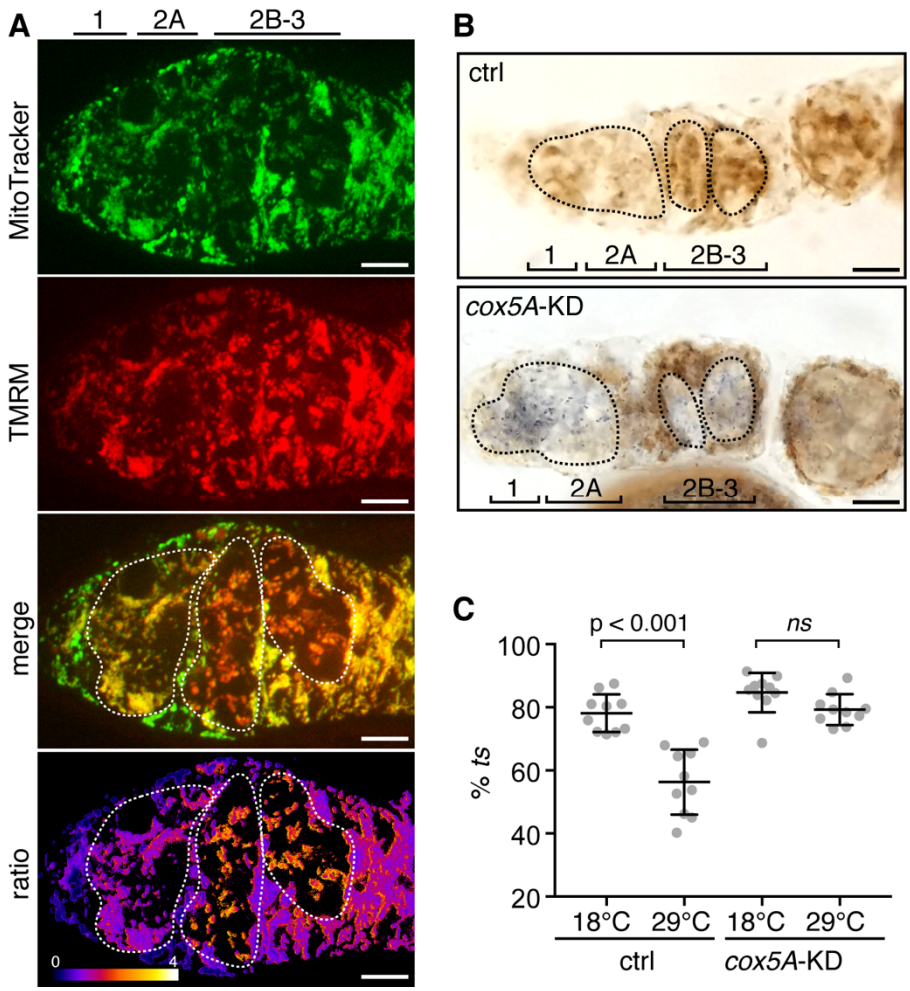

Figure 5. **Mitochondrial respiration is activated in 16-cell cyst and essential for mtDNA selective inheritance.** (A) Mitochondria activity staining demonstrated by the mitochondrial membrane indicator TMRM (red) and mitochondrial fluorescent dye mitoTracker (green). The strong red signal at region 2B and 3 in merged image suggests markedly increased membrane potential. The ratio of red to green fluorescence intensity is shown by the pseudo color radiometric image. The developing regions of germarium germ cells are outlined. Scale bar, 10 μm. (B) Ovaries from control and cox5A knockdown flies were stained for dual succinate dehydrogenase (complex II) and cytochrome C oxidase (complex IV) activity. Representative images for each group are shown. The complex IV activity is greatly reduced upon cox5A knockdown at all developmental stages of germarium. The developing regions of germarium germ cells are outlined. Scale bar, 10 μm. (C) Selection against the deleterious mtDNA mutation (*ts*) in heteroplasmic *mt:CoI*^{T300I} *Drosophila* is compromised by knocking down cox5A in the germline using nanos-gal4 driver. $p<0.001$.

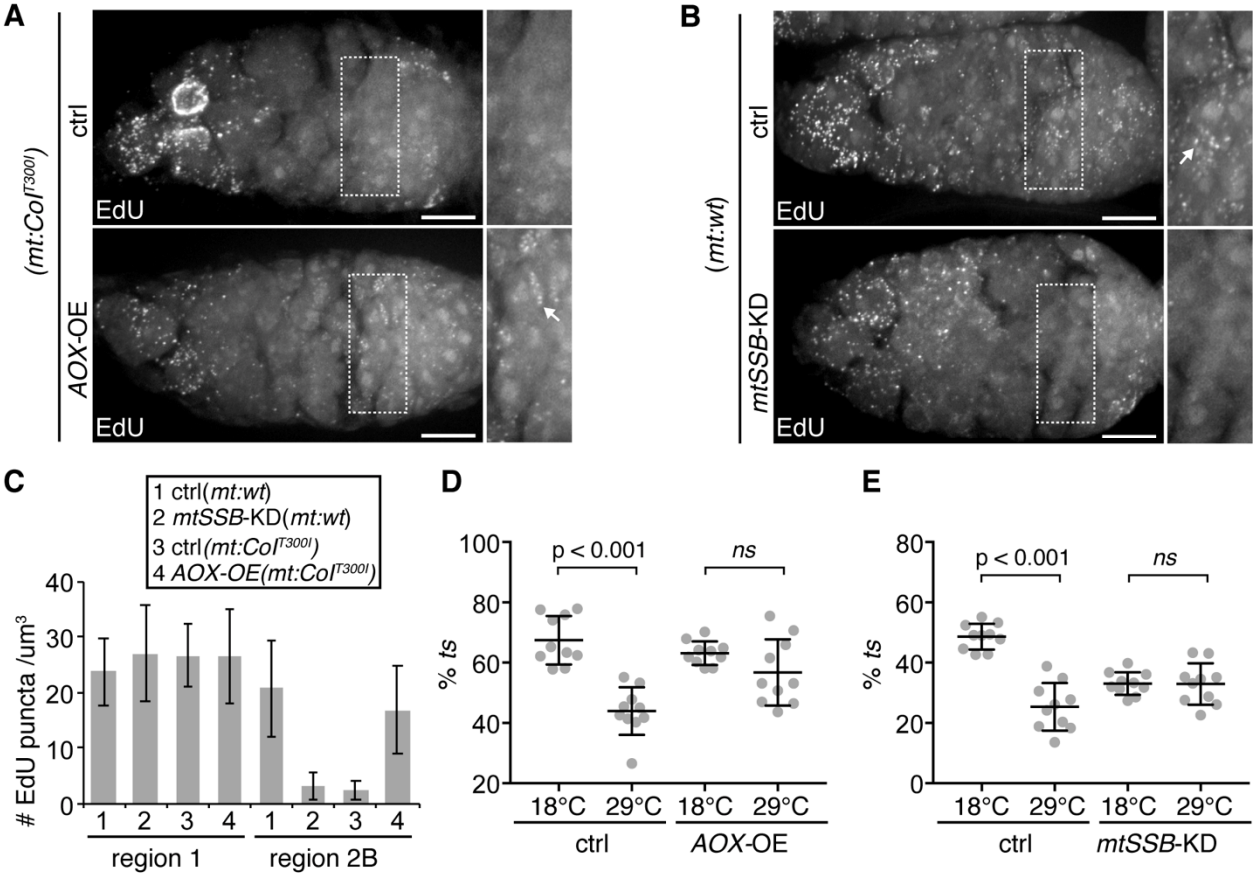

Figure 6. mtDNA replication are indispensable for selective inheritance. (A) and (B) mtDNA replication labeled by EdU staining in *Drosophila* germarium. Region 2B is outlined in white and enlarged on the right panels. Note that the mtDNA replication was specifically disrupted at region 2B in *mt:CoI^{T300I}* ovary at 29°C, but could be restored by overexpression of AOX (A). Knocking down mtSSB diminished mtDNA replication at region 2B of wild-type ovary (B). Arrows points to the EdU puncta. Scale bar, 10 μm. (C) Quantification of mtDNA replication indicated by numbers of EdU puncta in regions 1 and 2B in genetic backgrounds shown in (A) and (B). (D) and (E) Selection against *ts* mtDNA at 29°C is compromised by ectopic expression of AOX (D) and knocking down of mtSSB (E). $p<0.001$.

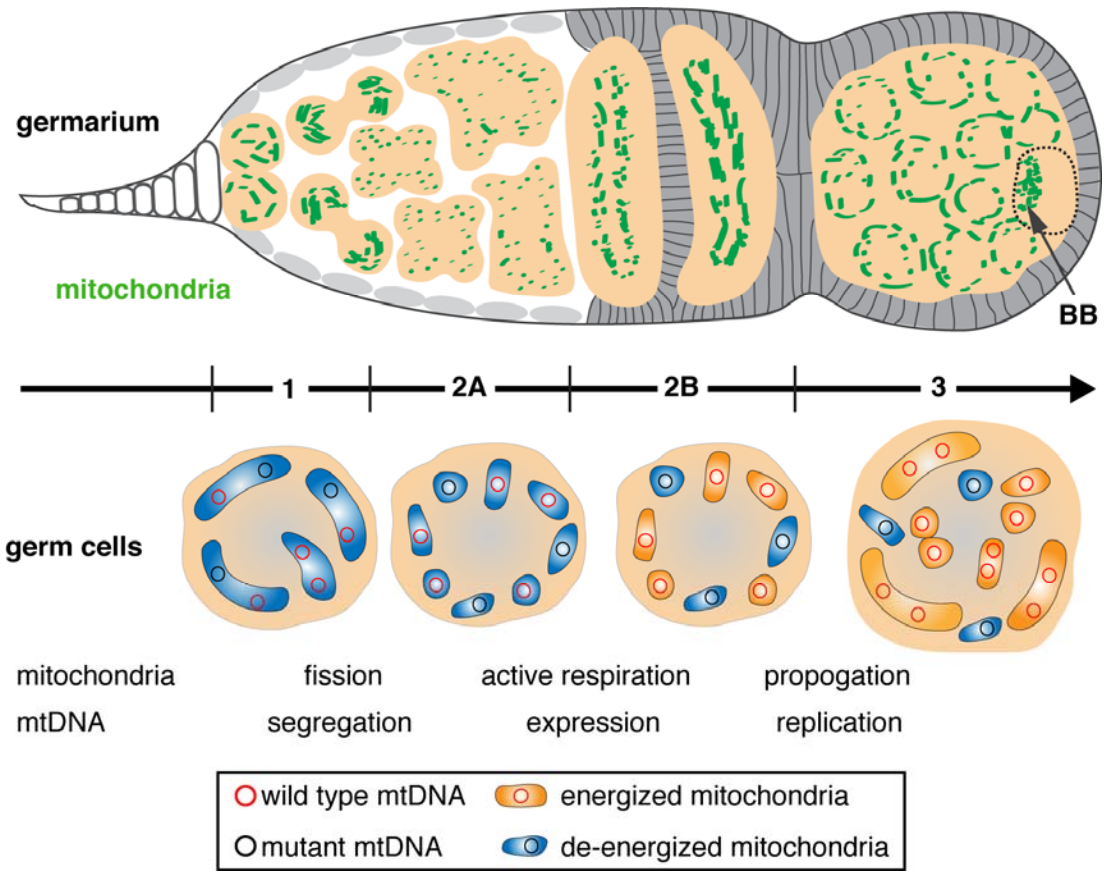

Figure 7. Mitochondria and mtDNA behaviors in the germarium of *Drosophila* are essential to limit the transmission of deleterious mutations. We propose that the mtDNA purifying selection is a developmentally regulated process. Mitochondrial fragmentation and mtDNA segregation in the developing cyst result in only one copy of mtDNA per mitochondrion, preparing for effective selection on the organelle level based on the functional readout of the mtDNA within. Mitochondrial respiration is boosted in 16-cell stage, revealing the phenotype of the mtDNA and allowing selection based on mitochondrial functionality. In late germarium stage, healthy mitochondria containing wild type mtDNA propagate much more vigorously than organelles containing deleterious mutations. These coordinated events act synergistically to secure the transmission of functional mtDNA from the female germline to the embryo. The Balbiani body (BB) in the oocyte further contributes to selective inheritance by concentrating wild-type mitochondria.

Supplemental Tables and Table Legends

Developmental stages	Wild type			Bam>Fis 1 RNAi		
	Mean	CV%	*n*	Mean	CV%	*n*
Region 1	1.91	34.2	24	1.82	38.6	24
Region 2A	1.09	26.4	12	1.62	42.8	12

Supplementary Table 1. Quantification of nucleoid numbers per mitochondrion in developing germarium region 1 and region 2A. CV, coefficient of variance; *n*, number of cells studied for each genotype.

	Progeny										
	1	2	3	4	5	6	7	8	9	10	Median
Mother 1	94.9	87.3	86.4	86	83.5	81.2	78.5	77.6	75.4	72.9	82.4
Mother 2	52.9	51.7	44.8	44.4	40.5	40	39.4	34	26.6	25.7	40.3
Mother 3	74.3	73.4	66	60.6	60	59.5	55.6	55.2	48.3	47.1	59.7
Mother 4	46.3	42.7	40.2	40	38.8	38.7	37	36.8	30	25	38.8
Mother 5	32.8	31.7	30.2	26.7	26.4	24.7	23	21.2	20.3	20.3	25.5
Mother 6	35.9	31.1	30.4	24.5	20.5	19.2	17	16.3	16	14	19.9
Mother 7	40.5	38	37.5	36.5	35	34.7	34.1	30.8	29.9	25.9	34.8
Mother 8	62	59.3	59.3	57.8	56.9	53.2	53.1	52	50.4	48.9	55.1
Mother 9	59.9	56.6	55	53.5	52.1	49.2	47.6	38.3	36.1	20.1	50.7
Mother 10	81.6	77.3	76.7	72.7	70	69.2	67.8	67.7	64.2	63.2	69.6
Mother 11	84.9	78.9	78.9	77.3	76.9	74.2	71.4	71.2	70.8	53.1	75.6
Mother 12	81.8	79.5	72.5	69.1	68.3	67.4	67.4	66.7	63.2	62.5	67.9
Mother 13	76.2	74.4	73	71.5	66.7	66.7	64.6	63.9	63.3	58.6	66.7
Mother 14	78.9	75.2	74.4	72	68	67.3	67.2	63.4	58.7	56.8	67.7
Mother 15	49	48.1	45.6	45.2	42.9	39.4	38.6				45.2
Mother 16	44.4	38.4	36.8	34.8	33.6	32.9	31.1	31	30.1	27.1	33.3
Mother 17	77.9	77.6	75.9	74.1	65.2	63.4	62.4	62.1	58.1	57.8	64.3
Mother 18	93.7	93.7	92.1	91.4	90.6	89.2	87.7	87.3	84.2	84	89.9
Mother 19	96.2	95.3	95.1	94.1	92.9	92.8	91.8	88.4			93.5
Mother 20	87.1	84.4	82.1	78.6	78.1	73.6	71.3	69	67.3	65.2	75.8

Supplementary Table 2. Proportion of mutant relative to wild-type mtDNA in progeny from 20 individual mother used for predicting mtDNA inheritance size in Table 2. Data are shown as % of total mtDNA population.

	p_A	V_n or V	N_{cd} or N
Model 1	0.5	5.45 x10^{-3}	45.9
Model 2	0.5	5.45 x10^{-3}	317.8

Supplementary Table 3. Predictions of the number of mitochondrial genetic segregation units during *Drosophila* germline development based on two mathematical models.
Model 1: $V_n = p_A (1-p_A)[1-(1-1/N_{cd})^{kn}]$
Model 2: $V = p_A (1-p_A)/N$

Supplementary Table 4. The sequence of fluorescence *in situ* hybridization short DNA probes targeting to *ND4*, *cox1*, *NDUFB5* and cox5A mRNA.